

# Exceptional twentieth-century slowdown in Atlantic Ocean overturning circulation

Stefan Rahmstorf<sup>1\*</sup>, Jason E. Box<sup>2</sup>, Georg Feulner<sup>1</sup>, Michael E. Mann<sup>3,4</sup>, Alexander Robinson<sup>1,5,6</sup>, Scott Rutherford<sup>7</sup> and Erik J. Schaffernicht<sup>1</sup>

**Possible changes in Atlantic meridional overturning circulation (AMOC) provide a key source of uncertainty regarding future climate change. Maps of temperature trends over the twentieth century show a conspicuous region of cooling in the northern Atlantic. Here we present multiple lines of evidence suggesting that this cooling may be due to a reduction in the AMOC over the twentieth century and particularly after 1970. Since 1990 the AMOC seems to have partly recovered. This time evolution is consistently suggested by an AMOC index based on sea surface temperatures, by the hemispheric temperature difference, by coral-based proxies and by oceanic measurements. We discuss a possible contribution of the melting of the Greenland Ice Sheet to the slowdown. Using a multi-proxy temperature reconstruction for the AMOC index suggests that the AMOC weakness after 1975 is an unprecedented event in the past millennium ( $p > 0.99$ ). Further melting of Greenland in the coming decades could contribute to further weakening of the AMOC.**

A persistent subpolar North Atlantic cooling anomaly is a conspicuous feature of the overall global warming pattern (Fig. 1). Model simulations indicate the largest cooling response to a weakening of the AMOC in this same region<sup>1</sup>, suggesting this area has so far defied global warming owing to a weakening of the AMOC over the past century. The time history of the AMOC over this period is poorly known, however, owing to the scarcity of direct measurements. Because of the large heat transport associated with the AMOC, changes in sea surface temperatures (SSTs) can be used as an indirect indicator of the AMOC evolution<sup>2</sup>.

Dima and Lohmann<sup>3</sup> identified two distinct modes in global SST evolution, one associated with a gradual decline of the global thermohaline circulation and one due to multidecadal and shorter AMOC variability, and concluded 'that the global conveyor has been weakening since the late 1930s and that the North Atlantic overturning cell suffered an abrupt shift around 1970'. Thompson *et al.*<sup>4</sup> found that the SST difference between the Northern and Southern Hemisphere underwent a sudden decline by  $\sim 0.5^\circ\text{C}$  around 1970, with the largest cooling observed over the northern Atlantic. We interpret this as indicative of a large-scale AMOC reduction, as the most plausible explanation for such a rapid change in the interhemispheric temperature difference is the cross-equatorial heat transport of the AMOC (ref. 5). Drijfhout *et al.*<sup>6</sup> regressed the AMOC strength and global-mean temperature on surface temperature fields in models and concluded that the conspicuous 'warming hole' south of Greenland is related to a weakening of the AMOC. They further found that a possible contribution of aerosol forcing to the cool patch as proposed in ref. 7 cannot be excluded.

Zhang *et al.*<sup>8</sup>, however, argue that the model simulation in ref. 7 overestimates the effect of aerosol forcing, by not accounting for

any increase in ocean heat content in the North Atlantic over the second half of the twentieth century, in contrast to what is suggested by the observations. The observational data show a clear dipole response in the Atlantic, with the North Atlantic cooling and the South Atlantic warming when comparing 1961–1980 with 1941–1960. The maximum of South Atlantic warming is within the Benguela Current off southern Africa and the maximum of North Atlantic cooling is found within the Gulf Stream. These patterns are highly characteristic of AMOC changes and are found in many model simulations wherein the AMOC is weakened by freshwater 'hosing experiments'. The Atlantic see-saw pattern is also evident in Fig. 1, where out of all Southern Hemisphere ocean regions the South Atlantic has warmed the most.

Terry<sup>9</sup> analysed the CMIP5 model ensemble together with observed SST data to quantify the relative contributions of radiatively forced changes to the total decadal SST variability. Although in most models forced changes explain more than half of the variance in low latitudes, they explain less than 10% in the subpolar North Atlantic, where in most cases their contribution is not significantly different from zero (the notable exception is the model used by Booth *et al.* as mentioned above).

To put the twentieth-century AMOC evolution into a longer-term context, in the following we develop an AMOC index based on surface temperatures from instrumental and proxy data.

## An AMOC index based on surface temperatures

We take the results of a climate model intercomparison<sup>1</sup> to identify the geographic region that is most sensitive to a reduction in the AMOC (Fig. 1), which for simplicity we henceforth refer to as 'subpolar gyre', although we use the term here merely to describe a geographic region and not an ocean circulation feature. To isolate the effect of AMOC changes from other climate change, we

<sup>1</sup>Potsdam Institute for Climate Impact Research (PIK), Earth System Analysis, Potsdam 14473, Germany. <sup>2</sup>Geologic Survey of Denmark and Greenland (GEUS), Østervoldgade 10, Copenhagen 1350, Denmark. <sup>3</sup>Pennsylvania State University, Department of Meteorology, University Park, Pennsylvania 16802, USA. <sup>4</sup>Environmental Systems Institute (ESI), University Park, Pennsylvania 16802, USA. <sup>5</sup>Universidad Complutense de Madrid, Dpto Astrofísica y CC de la Atmósfera, Madrid 28040, Spain. <sup>6</sup>Instituto de Geociencias, UCM-CSIC, Madrid 28040, Spain. <sup>7</sup>Department of Environmental Science, Roger Williams University, Bristol, Rhode Island 02809, USA. \*e-mail: stefan@pik-potsdam.de

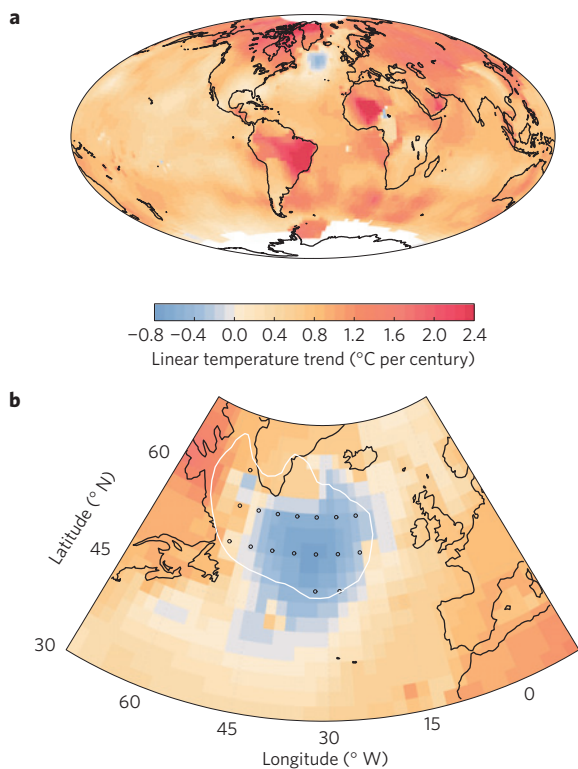


**Figure 1 | Linear trends of annual surface temperature since AD 1901.**

Based on the temperature data of NASA GISS (ref. 48). **a**, Global equal area map (Hammer projection) for 1901–2013; white indicates insufficient data. **b**, Same analysis for the North Atlantic sector for 1901–2000. In addition to the observed temperature trends **b** also shows the grid points (black circles) of the subpolar-gyre region for which time series are shown in Figs 3 and 5, as well as the model-average 2 °C cooling contour (white) from a climate model intercomparison<sup>1</sup> in which the models were subject to a strong AMOC reduction induced by adding a freshwater anomaly to the northern Atlantic. The geographic extent of the model-predicted temperature response to an AMOC reduction coincides well with the region of observed twentieth-century cooling. The models are forced more strongly and cooling extends further west as a result of shutting down Labrador Sea convection, which has only briefly happened in the real world so far. (Note that the second cooling patch in central Africa is in a region of poor data coverage and may be an artefact of data inhomogeneities.)

define an AMOC index by subtracting the Northern Hemisphere mean surface temperature from that of the subpolar gyre (see Supplementary Information for an alternative index obtained by subtracting Northern Hemisphere SST). We thus assume that differences in surface temperature evolution between the subpolar gyre and the whole Northern Hemisphere are largely due to changes in the AMOC. This seems to be a reasonable approximation in view of the evidence on North Atlantic SST variability discussed in the introduction. We decided against using an index based on a dipole between North and South Atlantic temperatures<sup>2,10</sup>, as this might be affected by the large gradient in aerosol forcing between both hemispheres.

We test the performance of the index in a global warming scenario experiment for 1850–2100 with a state-of-the-art global climate model, the MPI-ESM-MR. This model has a realistic representation of the AMOC (refs 10,11) based on criteria that include the magnitude and shape of the AMOC stream function and the realism of sites of deep-water formation. Without satisfying those criteria, we cannot expect realistic spatial patterns of SST response to AMOC variations and hence a good correlation of

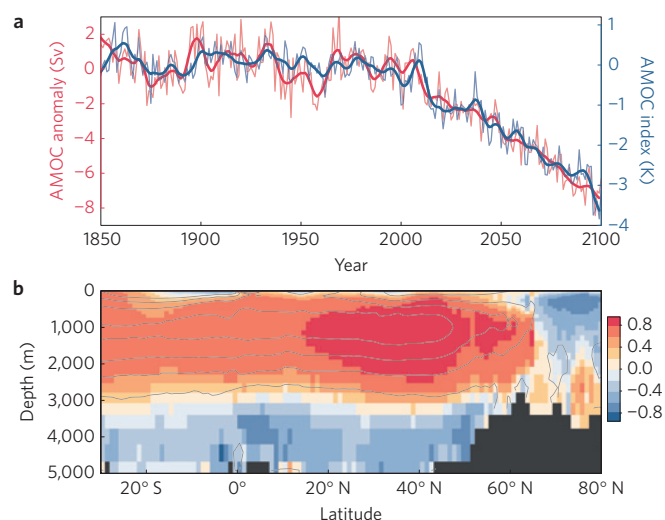


**Figure 2 | Connection between the AMOC stream function and the temperature-based AMOC index in a global warming scenario (RCP8.5).**

Simulated with the MPI-ESM-MR global climate model of the Max Planck Institute in Hamburg<sup>11</sup>. **a**, Time series of the maximum overturning stream function (red) and the AMOC index (blue). Thin lines show annual values, thick lines smoothed curves over 11 years. **b**, Correlation coefficient  $r$  of the overturning stream function in the model with the AMOC index (shading), shown together with the mean stream function (grey contours in 5 Sv intervals).

our temperature-based AMOC index with the actual AMOC. An analysis of ten global climate models found that a surface temperature response in the North Atlantic subpolar gyre is a robust feature of AMOC variability, although the details of this response depend on the quality of representation of the AMOC (ref. 10).

Figure 2 illustrates the high correlation of the AMOC index with the actual AMOC in the model, particularly on timescales of a decade and longer (smoothed curves). The correlation coefficient of the two smoothed curves after linear detrending is  $R=0.90$  and our temperature-based AMOC index predicts the actual AMOC changes in the model with an RMS error of 0.6 sverdrups (Sv; 1.1 Sv for the annual data), where the conversion factor of 2.3 Sv K<sup>-1</sup> has been fitted. Note that both individual components of the index—the subpolar gyre and the Northern Hemisphere surface temperature—increase during the twenty-first century in the simulation; it is the difference between the two which tracks the AMOC decline, as expected by our physical understanding of the effect of AMOC heat transport.

Figure 2b illustrates the correlation pattern of the AMOC stream function in the model with our AMOC index, exhibiting coherent large-scale structure that resembles the actual stream function (contoured). The circulation changes captured by the AMOC index are thus not local to the subpolar-gyre region but rather represent a large-scale response of the AMOC. Despite the good correlation with the AMOC in the model, our SST-based index only provides indirect evidence for possible AMOC changes.

### Reconstructing the AMOC index over the past millennium

To obtain a long-term reconstruction of the AMOC index requires long-term reconstructions of both the Northern Hemisphere mean temperature and SST of the subpolar gyre. For the Northern Hemisphere mean, Mann *et al.*<sup>12</sup> produced reconstructions using two different methods, composite-plus-scale (CPS) and errors in variables (EIV). Here we use the land-and-ocean reconstruction with the EIV method using all the available proxies, which is the reconstruction for which the best validation results were achieved

(see Supplementary Methods of Mann *et al.*<sup>12</sup>). Based on standard validation scores (Reduction of Error and Coefficient of Efficiency), this series provides a skilful reconstruction back to AD 900 and beyond (95% significance compared to a red-noise null).

The subpolar-gyre series is derived from a spatial temperature reconstruction<sup>13</sup>, which reconstructs land-and-ocean surface temperatures in every 5° latitude by 5° longitude grid box with sufficient instrumental data to perform calibration and validation. The subpolar gyre falls within the region where the individual grid-box reconstructions are assessed to be skilful compared to a red-noise null<sup>13</sup>. In addition, we performed validation testing of the subpolar-gyre mean series, which indicates a skilful reconstruction back to AD 900 (95% significance compared to a red-noise null; see Supplementary Information for details).

Both time series as well as the resulting AMOC index are shown in Fig. 3. Remarkably, the subpolar gyre reaches nearly its lowest temperatures of the past millennium in the late twentieth century (orange curve), despite global warming. Mann *et al.*<sup>13</sup> already noted that this region near Greenland is anomalous in being colder during the modern reference period (1961–1990) than even in the Little Ice Age (LIA). The AMOC index (blue curve) indicates a steady AMOC, with modest changes until the beginning of the twentieth century. There is indication of a maximum in the fifteenth century and a minimum around AD 1600. There is no sign in our index that a weak AMOC caused the LIA in the Northern Hemisphere<sup>14</sup>; rather the data are consistent with previous findings that the LIA reflects a response to natural volcanic and solar forcing<sup>15–17</sup>, and if anything this surface cooling strengthened the AMOC at least during the first part of the LIA. The fact that LIA coldness seems to have been even more pronounced in South America than in Europe<sup>18</sup> further argues against a weak AMOC, as the latter would have warmed the Southern Hemisphere. The twentieth century shows a gradual decline in the AMOC index, followed by a sharp drop starting around 1970 with a partial recovery after 1990 (discussed further below). This recovery is consistent with the finding of an AMOC increase since 1993 based on floats and satellite altimeter data<sup>19</sup>.

Our temperature reconstruction for the subpolar gyre differs from three estimates based on ocean sediment cores from the region<sup>20,21</sup>. However, reconciling these cores with each other and with the instrumental SST record proves problematic (see Supplementary Information), whereas our reconstruction compares well with the instrumental data during the period of overlap.

Spectral analysis<sup>50</sup> of the AMOC index indicates a few marginally significant peaks with periods around 22, 27 and 37 years, but these features are not clearly discernible from the expectations of simple red noise (Fig. 4). We find no significant peak in the 50–70-year period range although our index should pick this up<sup>10</sup>, suggesting that the ‘Atlantic Multidecadal Oscillation’ (AMO) described in previous studies<sup>22–24</sup> is not a prominent feature of our AMOC index time series.

### The twentieth-century AMOC weakening

The most striking feature of the AMOC index is the extremely low index values reached from 1975 to 1995. It is primarily this negative anomaly that yields the cooling patch in the trend maps illustrated in Fig. 1. In the following we discuss this downward spike in more detail.

The significance of the 1975–1995 AMOC index reduction was estimated using a Monte Carlo method (see Supplementary Information). The annually resolved AMOC reconstruction from 900 to 1850 formed the basis for an ARMA(1,1) model which closely resembles the statistical properties of the data. 10,000 simulated time series of the same length as the AMOC index were constructed. The probability of reaching a similarly weak AMOC index as during 1975–1995 just by natural variability was

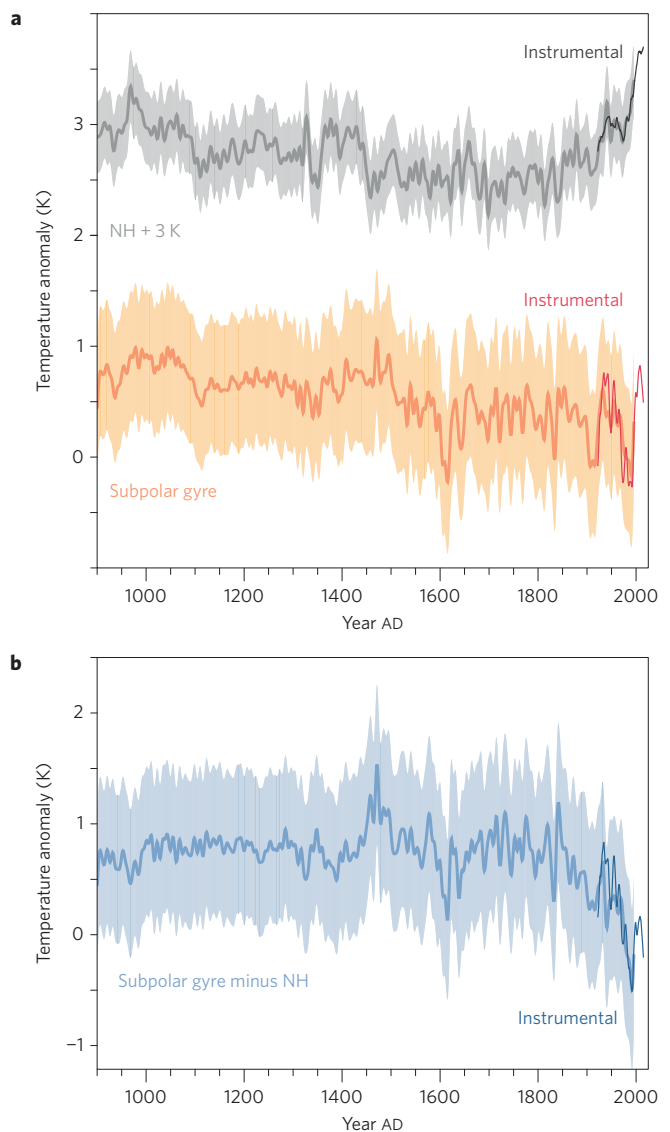


**Figure 3 | Surface temperature time series for different regions.** Data from the proxy reconstructions of Mann *et al.*<sup>12,13</sup>, including estimated  $2\text{-}\sigma$  uncertainty bands, and from the HadCRUT4 instrumental data<sup>49</sup>. The latter are shown in darker colours and from 1922 onwards, as from this time on data from more than half of all subpolar-gyre grid cells exist in every month (except for a few months during World War II). The orange/red curves are averaged over the subpolar gyre, as indicated on Fig. 1. The grey/black curves are averaged over the Northern Hemisphere, offset by 3 K to avoid overlap. The blue curves in the bottom panel show our AMOC index, namely the difference between subpolar gyre and Northern Hemisphere temperature anomalies (that is, orange/red curves minus grey/black curves). Proxy and instrumental data are decadal smoothed.

found to be  $<0.005$ , based on the uncertainty of the proxy data and ignoring that this weakening is independently supported by instrumental data.

Figure 5 illustrates corroborating evidence in support of a twentieth-century AMOC weakening. The blue curve depicts the AMOC index from Fig. 3. The dark red curve illustrates the corresponding index based on the instrumental NASA GISS global temperature analysis. The green curve denotes oceanic nitrogen-15 proxy data from corals off the US north-east coast from ref. 25. These annually resolved  $\delta^{15}\text{N}$  data represent a tracer for water mass changes in the region, where high values are characteristic

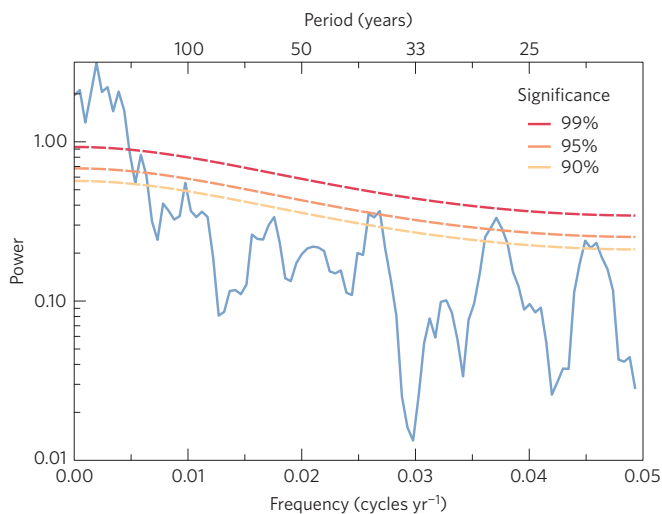


**Figure 4 | Spectral analysis of the proxy-based AMOC index shown in Fig. 3b.**

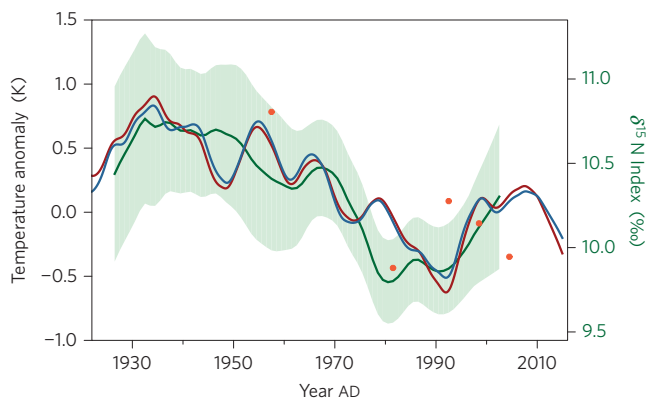


**Figure 5 | A compilation of different indicators for Atlantic ocean circulation.** The blue curve shows our temperature-based AMOC index also shown in Fig. 3b. The dark red curve shows the same index based on NASA GISS temperature data<sup>48</sup> (scale on left). The green curve with uncertainty range shows coral proxy data<sup>25</sup> (scale on right). The data are decadal smoothed. Orange dots show the analyses of data from hydrographic sections across the Atlantic at 25° N, where a 1 K change in the AMOC index corresponds to a 2.3 Sv change in AMOC transport, as in Fig. 2 based on the model simulation. Other estimates from oceanographic data similarly suggest relatively strong AMOC in the 1950s and 1960s, weak AMOC in the 1970s and 1980s and stronger again in the 1990s (refs 41,51).

of the presence of Labrador Slope Water. The time evolution of the  $\delta^{15}\text{N}$  tracer agrees well with that of our AMOC index (Fig. 5). Ref. 25 reports four more data points from ancient corals preceding the twentieth century, the oldest one from AD  $\sim 500$ . These lie all above 10.5‰, providing (albeit limited) evidence that the downward excursion to values below 10‰ between 1975 and 1995 and the corresponding water mass change may be unprecedented in several centuries.

Finally, Fig. 5 includes data points from repeat hydrographic sections across the Atlantic at 25° N, from which ref. 26 originally concluded that the AMOC had slowed by 30% since the 1950s. These measurements were later adjusted for seasonal variations<sup>27</sup> and are shown in this form here; recent observations over 2004–2012 show inter-annual variability<sup>28</sup> with a standard deviation of 1.7 Sv, which needs to be kept in mind.

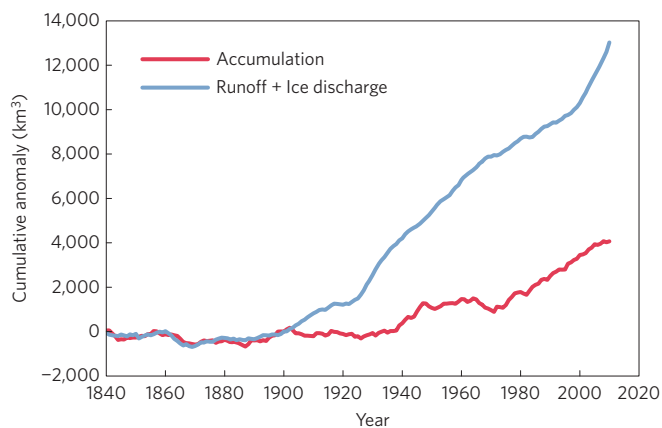


**Figure 6 | Mass balance terms of the Greenland Ice Sheet.** Data from Box and Colgan<sup>33</sup>. Cumulative anomaly relative to the mean over 1840–1900, a pre-industrial period during which the Greenland Ice Sheet was approximately in balance.

### Causes of the weakening and implications for the future

Because the AMOC is driven by density gradients related to deep-water formation in the high-latitude North Atlantic, a weakening of the AMOC could be caused by a regional reduction in surface ocean density. Ref. 29 describes an ongoing freshening trend in the northern Atlantic in which the net freshwater storage increased by 19,000 km<sup>3</sup> between 1961 and 1995, and the rapid AMOC drop in 1970 was preceded by a large-scale freshening known as the Great Salinity Anomaly<sup>30,31</sup>. This freshwater anomaly was described in 1988 as ‘one of the most persistent and extreme variations in global ocean climate yet observed in this century’<sup>31</sup>, the source of which has been linked to anomalous sea-ice export from the Arctic Ocean<sup>30,31</sup>. The freshwater volume anomaly of the Great Salinity Anomaly has been estimated as 2,000 km<sup>3</sup> along the Labrador coast<sup>30,31</sup>.

Additional sources of freshwater addition are increasing river discharge into the Arctic Ocean<sup>32</sup> and meltwater and iceberg discharge from the Greenland Ice Sheet (GIS). Because surface flow is directed northward and freshwater tends to remain near the surface owing to its low density, it is difficult to remove freshwater from the northern Atlantic, so an accumulation over longer timescales is plausible. According to a recent reconstruction of the total GIS mass balance from AD 1840 (ref. 33), the GIS was close to balance in the nineteenth century, but a persistent mass loss from Greenland began in AD 1900. The cumulative runoff and ice discharge anomaly (relative to the mean over 1840–1900) during AD 1900–1970 is estimated as 8,000 km<sup>3</sup>, of which 1,800 km<sup>3</sup> was released after 1955 (Fig. 6). It is thus plausible that the accumulated freshwater input from Greenland may have made a significant contribution to the observed freshening trend. A comparable Southern Ocean freshening has likewise been linked to Antarctic ice sheet mass loss<sup>34</sup>.

This dilution of the surface ocean could have weakened deep-water formation, slowing the AMOC. A shutdown of deep convection in the Labrador Sea from 1969 to 1971 is well documented<sup>35</sup> and the stability of Labrador Sea convection has been the subject of a number of studies<sup>36,37</sup>. Perhaps as a consequence of the cooling in the Greenland region starting in 1970, the GIS subsequently was closer to mass balance for three decades until AD  $\sim 2000$  (ref. 33). Since then the GIS has started to lose mass again at a rapidly increasing rate, consistent with the surface warming of the region which has been attributed to a recovery of the AMOC based on model simulations initialized with observations<sup>38</sup>. This recovery is also seen in the AMOC index proposed in Fig. 5.

Recent oceanographic measurements from the RAPID array at 26° N in the Atlantic suggest that the AMOC has been weakening again since these measurements started in 2004 (ref. 39), although we cannot conclude to what extent this temporary decrease signals a progressive trend, and the connection between subtropical and subpolar overturning, especially on shorter timescales, is not clear<sup>40</sup>.

Climate models from the CMIP5 ensemble forced by natural and anthropogenic forcings generally show a much weaker subpolar cooling than the observations<sup>6</sup> and do not capture the observed North Atlantic subpolar cooling during 1970–1990, even though they show a much smaller and more short-lived cooling following the Agung eruption in 1963/1964 (ref. 9). The failure of the models to capture the cooling is probably not due to an underestimation of the response to the Agung eruption, as volcanic cooling would if anything strengthen the AMOC, whereas the data indicate an AMOC weakening<sup>41</sup>. Rather, this failure suggests that these models either have an AMOC that is too stable with respect to buoyancy forcing<sup>42,43</sup>, or are missing an important forcing (and indeed the time history of Greenland meltwater runoff is not included as a forcing in the CMIP5 ensemble).

Although major uncertainties remain about the past evolution of the AMOC for lack of direct measurements, indirect evidence from multiple sources provides a consistent picture, linking together the time evolution of surface temperature, ocean circulation and, possibly, Greenland ice mass balance. If the interconnections between these three components continue as we have conjectured, the ongoing melting of the GIS, which reached an extreme in 2012 (ref. 44), may lead to further freshening of the subpolar Atlantic in the next few decades. Bamber *et al.*<sup>45</sup> estimate that if current trends continue, the Greenland freshwater input from 1995 to AD 2025 may exceed 10,000 km<sup>3</sup>. This might lead to further weakening of the AMOC within a decade or two, and possibly even more permanent shutdown of Labrador Sea convection as a result of global warming, as has been predicted by some climate models<sup>46,47</sup>.

Received 14 July 2014; accepted 28 January 2015;  
published online 23 March 2015; corrected after print  
3 September 2015

## References

- Stouffer, R. *et al.* Investigating the causes of the response of the thermohaline circulation to past and future climate changes. *J. Clim.* **19**, 1365–1387 (2006).
- Latif, M. *et al.* Reconstructing, monitoring, and predicting multidecadal-scale changes in the North Atlantic thermohaline circulation with sea surface temperature. *J. Clim.* **17**, 1605–1614 (2004).
- Dima, M. & Lohmann, G. Evidence for two distinct modes of large-scale ocean circulation changes over the last century. *J. Clim.* **23**, 5–16 (2010).
- Thompson, D. W. J., Wallace, J. M., Kennedy, J. J. & Jones, P. D. An abrupt drop in Northern Hemisphere sea surface temperature around 1970. *Nature* **467**, 444–447 (2010).
- Feulner, G., Rahmstorf, S., Levermann, A. & Volkwardt, S. On the origin of the surface air temperature difference between the hemispheres in Earth's present-day climate. *J. Clim.* **26**, 7136–7150 (2013).
- Drijfhout, S., van Oldenborgh, G. J. & Cimadoribus, A. Is a decline of AMOC causing the warming hole above the North Atlantic in observed and modeled warming patterns? *J. Clim.* **25**, 8373–8379 (2012).
- Booth, B. B. B., Dunstone, N. J., Halloran, P. R., Andrews, T. & Bellouin, N. Aerosols implicated as a prime driver of twentieth-century North Atlantic climate variability. *Nature* **484**, 228–232 (2012).
- Zhang, R. *et al.* Have aerosols caused the observed Atlantic multidecadal variability? *J. Atmos. Sci.* **70**, 1135–1144 (2013).
- Terray, L. Evidence for multiple drivers of North Atlantic multi-decadal climate variability. *Geophys. Res. Lett.* **39**, L19712 (2012).
- Roberts, C. D., Garry, F. K. & Jackson, L. C. A multimodel study of sea surface temperature and subsurface density fingerprints of the Atlantic meridional overturning circulation. *J. Clim.* **26**, 9155–9174 (2013).
- Jungclauss, J. H. *et al.* Characteristics of the ocean simulations in the Max Planck Institute Ocean Model (MPIOM) the ocean component of the MPI-Earth system model. *J. Adv. Model. Earth Syst.* **5**, 422–446 (2013).
- Mann, M. E. *et al.* Proxy-based reconstructions of hemispheric and global surface temperature variations over the past two millennia. *Proc. Natl Acad. Sci. USA* **105**, 13252–13257 (2008).
- Mann, M. E. *et al.* Global signatures and dynamical origins of the Little Ice Age and Medieval Climate Anomaly. *Science* **326**, 1256–1260 (2009).
- Wanmaker, A. *et al.* Surface changes in the North Atlantic meridional overturning circulation during the last millennium. *Nature Commun.* **3**, 899 (2012).
- Crowley, T. J. Causes of climate change over the past 1000 years. *Science* **289**, 270–277 (2000).
- Shindell, D. T., Schmidt, G. A., Miller, R. L. & Mann, M. E. Volcanic and solar forcing of climate change during the preindustrial era. *J. Clim.* **16**, 4094–4107 (2003).
- Feulner, G. Are the most recent estimates for Maunder Minimum solar irradiance in agreement with temperature reconstructions? *Geophys. Res. Lett.* **38**, L16706 (2011).
- PAGES 2k Consortium Continental-scale temperature variability during the past two millennia. *Nature Geosci.* **6**, 339–346 (2013).
- Willis, J. Can *in situ* floats and satellite altimeters detect long-term changes in Atlantic Ocean overturning? *Geophys. Res. Lett.* **37**, L06602 (2010).
- Moffa-Sanchez, P., Born, A., Hall, I. R., Thornalley, D. J. R. & Barker, S. Solar forcing of North Atlantic surface temperature and salinity over the past millennium. *Nature Geosci.* **7**, 275–278 (2014).
- Miettinen, A., Divine, D., Koc, N., Godtliebsen, F. & Hall, I. R. Multicentennial variability of the sea surface temperature gradient across the subpolar North Atlantic over the last 2.8 kyr. *J. Clim.* **25**, 4205–4219 (2012).
- Delworth, T. L. & Mann, M. E. Observed and simulated multidecadal variability in the Northern Hemisphere. *Clim. Dynam.* **16**, 661–676 (2000).
- Chambers, D. P., Merrifield, M. A. & Nerem, R. S. Is there a 60-year oscillation in global mean sea level? *Geophys. Res. Lett.* **39**, L18607 (2012).
- Tung, K. & Zhou, J. Using data to attribute episodes of warming and cooling in instrumental records. *Proc. Natl Acad. Sci. USA* **110**, 2058–2063 (2013).
- Sherwood, O. A., Lehmann, M. F., Schubert, C. J., Scott, D. B. & McCarthy, M. D. Nutrient regime shift in the western North Atlantic indicated by compound-specific delta N-15 of deep-sea gorgonian corals. *Proc. Natl Acad. Sci. USA* **108**, 1011–1015 (2011).
- Bryden, H. L., Longworth, H. R. & Cunningham, S. A. Slowing of the Atlantic meridional overturning circulation at 25° N. *Nature* **438**, 655–657 (2005).
- Kanzow, T. *et al.* Seasonal variability of the Atlantic Meridional overturning circulation at 26.5° N. *J. Clim.* **23**, 5678–5698 (2010).
- Smeed, D. A. *et al.* Observed decline of the Atlantic meridional overturning circulation 2004–2012. *Ocean Sci.* **10**, 29–38 (2014).
- Curry, R. & Mauritzen, C. Dilution of the northern North Atlantic Ocean in recent decades. *Science* **308**, 1772–1774 (2005).
- Belkin, I. M., Levitus, S., Antonov, J. & Malmberg, S.-A. “Great Salinity Anomalies” in the North Atlantic. *Prog. Oceanogr.* **41**, 1–68 (1998).
- Dickson, R. R., Meincke, J., Malmberg, S. A. & Lee, A. J. The “Great Salinity Anomaly” in the northern North Atlantic, 1968–82. *Prog. Oceanogr.* **20**, 103–151 (1988).
- Peterson, B. J. *et al.* Increasing river discharge to the Arctic Ocean. *Science* **298**, 2171–2173 (2002).
- Box, J. & Colgan, W. Greenland Ice Sheet mass balance reconstruction. Part III: Marine ice loss and total mass balance (1840–2010). *J. Clim.* **26**, 6990–7002 (2013).
- Rye, C. *et al.* Rapid sea-level rise along the Antarctic margins in response to increased glacial discharge. *Nature Geosci.* **7**, 732–735 (2014).
- Lazier, J. R. N. Oceanographic conditions at Ocean Weather Ship *Bravo*, 1964–74. *Atmos.-Ocean* **18**, 227–238 (1980).
- Kuhlbrodt, T., Titz, S., Feudel, U. & Rahmstorf, S. A simple model of seasonal open ocean convection. Part II: Labrador Sea stability and stochastic forcing. *Ocean Dynam.* **52**, 36–49 (2001).
- Gelderloos, R., Straneo, F. & Katsman, C. A. Mechanisms behind the temporary shutdown of deep convection in the Labrador Sea: Lessons from the great salinity anomaly years 1968–71. *J. Clim.* **25**, 6743–6755 (2012).
- Robson, J. I., Sutton, R. T. & Smith, D. M. Initialized decadal predictions of the rapid warming of the North Atlantic Ocean in the mid 1990s. *Geophys. Res. Lett.* **39**, L19713 (2012).
- Robson, J., Hodson, D., Hawkins, E. & Sutton, R. Atlantic overturning in decline? *Nature Geosci.* **7**, 2–3 (2014).
- Lozier, M. S., Roussenov, V., Reed, M. S. C. & Williams, R. G. Opposing decadal changes for the North Atlantic meridional overturning circulation. *Nature Geosci.* **3**, 728–734 (2010).
- Zhang, R. Coherent surface-subsurface fingerprint of the Atlantic meridional overturning circulation. *Geophys. Res. Lett.* **35**, L20705 (2008).

42. Hofmann, M. & Rahmstorf, S. On the stability of the Atlantic meridional overturning circulation. *Proc. Natl Acad. Sci. USA* **106**, 20584–20589 (2009).
43. Weaver, A. J. *et al.* Stability of the Atlantic meridional overturning circulation: A model intercomparison. *Geophys. Res. Lett.* **39**, L20709 (2012).
44. Nghiem, S. V. *et al.* The extreme melt across the Greenland Ice Sheet in 2012. *Geophys. Res. Lett.* **39**, L20502 (2012).
45. Bamber, J., van den Broeke, M., Ettema, J., Lenaerts, J. & Rignot, E. Recent large increases in freshwater fluxes from Greenland into the North Atlantic. *Geophys. Res. Lett.* **39**, L19501 (2012).
46. Rahmstorf, S. Shifting seas in the greenhouse? *Nature* **399**, 523–524 (1999).
47. Wood, R. A., Keen, A. B., Mitchell, J. F. B. & Gregory, J. M. Changing spatial structure of the thermohaline circulation in response to atmospheric CO<sub>2</sub> forcing in a climate model. *Nature* **399**, 572–575 (1999).
48. Hansen, J., Ruedy, R., Glascoe, J. & Sato, M. GISS analysis of surface temperature change. *J. Geophys. Res.* **104**, 30997–31022 (1999).
49. Morice, C. P., Kennedy, J. J., Rayner, N. A. & Jones, P. D. Quantifying uncertainties in global and regional temperature change using an ensemble of observational estimates: The HadCRUT4 data set. *J. Geophys. Res.* **117**, D08101 (2012).
50. Mann, M. E. & Lees, J. M. Robust estimation of background noise and signal detection in climatic time series. *Climatic Change* **33**, 409–445 (1996).
51. Huck, T., Colin de Verdiere, A., Estrade, P. & Schopp, R. Low-frequency variations of the large-scale ocean circulation and heat transport in the North Atlantic from 1955–1998 *in situ* temperature and salinity data. *Geophys. Res. Lett.* **35**, L23613 (2008).

### Acknowledgements

We thank O. Sherwood for providing coral data. M.E.M. acknowledges support for this work from the ATM program of the National Science Foundation (grant ATM-0902133).

### Author contributions

S.Rahmstorf conceived and designed the research and wrote the paper, E.J.S., S.Rutherford, A.R. and G.F. performed the research, M.E.M. and J.E.B. contributed materials/analysis tools and co-wrote the paper.

### Additional information

Supplementary information is available in the [online version of the paper](#). Reprints and permissions information is available online at [www.nature.com/reprints](http://www.nature.com/reprints). Correspondence and requests for materials should be addressed to S.Rahmstorf

### Competing financial interests

The authors declare no competing financial interests.

## Corrigendum: Evidence for an exceptional twentieth-century slowdown in Atlantic Ocean overturning

Stefan Rahmstorf, Jason Box, Georg Feulner, Michael E. Mann, Alexander Robinson, Scott Rutherford and Erik Schaffernicht

*Nature Clim. Change* 5, 475–480 (2015); published online 23 March 2015; corrected after print 3 September 2015

In the version of this Article originally published, in Fig. 1 the data plotted were for the calendar month of December and not the annual mean data. This has been replaced with a new global temperature trend map for annual mean data, in which (due to the reduced variability of annual as compared with monthly data) the cooling patch in the subpolar North Atlantic stands out even more. The first sentence of the caption for Fig. 1 has been amended to: 'Linear trends of annual surface temperature since AD 1901'. None of the conclusions in the Article are affected by this error.